

Experimental constraints on the $^{73}\text{Zn}(n, \gamma)^{74}\text{Zn}$ reaction rate

R. Lewis,^{1,2,*} S. N. Liddick,^{1,2} A. C. Larsen,³ A. Spyrou,^{1,4,5} D. L. Bleuel,⁶ A. Couture,⁷ L. Crespo Campo,³
 B. P. Crider,^{1,8} A. C. Dombos,^{1,4,5} M. Guttormsen,³ S. Mosby,⁷ F. Naqvi,¹ G. Perdikakis,^{9,1,5}
 C. J. Prokop,^{1,2} S. J. Quinn,^{1,4,5} T. Renström,³ and S. Siem³

¹*National Superconducting Cyclotron Laboratory, Michigan State University, East Lansing, MI 48824, USA*

²*Department of Chemistry, Michigan State University, East Lansing, MI 48824, USA*

³*Department of Physics, University of Oslo, N-0316 Oslo, Norway*

⁴*Department of Physics and Astronomy, Michigan State University, East Lansing, MI 48824, USA*

⁵*Joint Institute for Nuclear Astrophysics, Michigan State University, East Lansing, MI 48824, USA*

⁶*Lawrence Livermore National Laboratory, Livermore, CA 94550, USA*

⁷*Los Alamos National Laboratory, Los Alamos, NM 87545, USA*

⁸*Department of Physics and Astronomy, Mississippi State University, Mississippi State, MS 39762, USA*

⁹*Central Michigan University, Mount Pleasant, MI 48859, USA*



(Received 21 September 2018; published 1 March 2019)

Background: The recent observation of a neutron-star merger finally confirmed one astrophysical location of the rapid neutron-capture process (r-process). Evidence of the production of $A < 140$ nuclei was seen, but there is still little detailed information about how those lighter elements are produced in such an environment. Many of the questions surrounding the $A \approx 80$ nuclei are likely to be answered only when the nuclear physics involved in the production of r-process nuclei is well understood. Neutron-capture reactions are an important component of the r-process, and neutron-capture cross sections of r-process nuclei, which are very neutron rich, have large uncertainties.

Purpose: Indirectly determine the neutron-capture cross section and reaction rate of $^{73}\text{Zn}(n, \gamma)^{74}\text{Zn}$.

Methods: The nuclear level density (NLD) and γ -ray strength function (γ SF) of ^{74}Zn were determined following a total absorption spectroscopy (TAS) experiment focused on the β decay of ^{74}Cu into ^{74}Zn performed at the National Superconducting Cyclotron Laboratory. The NLD and γ SF were used as inputs in a Hauser-Feshbach statistical model to calculate the neutron-capture cross section and reaction rate.

Results: The NLD and γ SF of ^{74}Zn were experimentally constrained for the first time using β -delayed γ rays measured with TAS and the β -Oslo method. The NLD and γ SF were then used to constrain the neutron-capture cross section and reaction rate for the $^{73}\text{Zn}(n, \gamma)^{74}\text{Zn}$ reaction.

Conclusions: The uncertainty in the neutron-capture cross section and reaction rate of $^{73}\text{Zn}(n, \gamma)^{74}\text{Zn}$ calculated in TALYS was reduced to under a factor of 2 from a factor of 5 in the cross section and a factor of 11 in the reaction rate using the experimentally obtained NLD and γ SF.

DOI: [10.1103/PhysRevC.99.034601](https://doi.org/10.1103/PhysRevC.99.034601)

I. INTRODUCTION

The production of the elements heavier than iron involves processes that require neutron-capture reactions. The slow neutron-capture process (s-process) and rapid neutron-capture process (r-process) are the most well known and are thought to account for the production of the majority of the heavy elements [1,2]. The r-process in particular is characterized by successive neutron captures on neutron-rich, unstable nuclei, which is possible due to the high neutron flux assumed in such a process. Neutron-star mergers have recently been identified as one site of the r-process through electromagnetic observations of a kilonova afterglow that indicated the presence of r-process nuclei (see e.g., Refs. [3,4]). Even with this new information, the question of where r-process nuclei are made

is not settled. This is partly due to the indication that there may be multiple processes involved in producing r-process nuclei, such as the weak r-process [5,6] and the intermediate neutron-capture process (i-process) [7]. This is especially important when considering nuclei in the $A \approx 80$ region, where the abundance pattern observed in various metal-poor stars is not as robust as it is for heavier elements [8].

Understanding the production of the $A \approx 80$ elements requires models of astrophysical processes that combine large-scale astrophysics information with detailed nuclear physics information. Nuclear properties such as β -decay half-lives, masses, fission properties, and neutron-capture rates all impact predicted r-process abundances [9,10]. Neutron-capture cross sections relevant for r-process nucleosynthesis are particularly difficult to obtain experimentally, due to the short half-lives of the nuclei involved in the neutron-capture reaction and the free neutron. Theoretical neutron-capture cross sections can be obtained using a Hauser-Feshbach model and

*lewis@nscl.msu.edu

a knowledge of the optical model potential (OMP), nuclear level density (NLD), and γ -ray strength function (γ SF) [11]. The NLD describes the number of levels as a function of excitation energy while the γ SF describes the likelihood that a γ ray of a given energy will be emitted from the nucleus. However, the extrapolation of the NLD and γ SF are uncertain as a progression is made to short-lived nuclei [12,13], leading to a variation of theoretically calculated neutron-capture cross sections that can quickly approach orders of magnitude just a few nucleons away from stable isotopes [14]. The β -Oslo method [15] is one of a few indirect techniques [16–18] used to inform our knowledge of neutron-capture cross sections on short-lived isotopes. The β -Oslo method provides statistical properties of the nucleus—the NLD and γ SF—that can be used to calculate a neutron-capture cross section using the Hauser-Feshbach model.

The $^{73}\text{Zn}(n, \gamma)^{74}\text{Zn}$ cross section was identified in a sensitivity study to have an influence on the predicted abundance pattern in the $A \approx 80$ region [6]. The astrophysical reaction rate calculated in TALYS [19,20], a widely used Hauser-Feshbach model code, can be uncertain by a factor of 11 by varying the included NLD and γ SF models. The cross section is also uncertain up to a factor of 5. This large uncertainty inherent to model choice has been seen in the $A \approx 70$ region to increase quickly just a few neutrons from stability [14]. The neutron-capture cross section and reaction rate of the $^{73}\text{Zn}(n, \gamma)^{74}\text{Zn}$ reaction were constrained by experimentally determining the NLD and γ SF of ^{74}Zn following the β decay of ^{74}Cu , reducing the uncertainty in each to under a factor of 2.

II. EXPERIMENT

The experiment was performed at the National Superconducting Cyclotron Laboratory at Michigan State University. A beam of ^{86}Kr was accelerated to 140 MeV/nucleon and fragmented on a 376 mg/cm² Be target. Ions of ^{74}Cu were separated in the A1900 fragment separator [21] and sent to the experimental end station as part of a cocktail beam of approximately 10 nuclei [14,22,23]. The experimental setup consisted of the Summing NaI (SuN) detector [24], a Si double sided strip detector (DSSD), a Si veto detector, and two Si PIN detectors. SuN is cylindrical, 16 inches in height and diameter, with a 1.7-inch borehole along the beam axis, and is separated into eight optically isolated segments [15]. The DSSD was placed in the center of the borehole and was used to stop and detect the ions. The veto detector was placed just downstream of the DSSD, and in the borehole of SuN, for the detection of any light particles that did not stop in the DSSD. The PIN detectors were placed just upstream of SuN.

The DSSD had a set of 16 strips, each 1.2 mm wide, on the front and back faces, arranged perpendicularly to each other to obtain position information on both the implanted ion and the β -decay electron. The β -decay electrons were correlated to the previously stopped ion based on timing and position information. γ rays following the β decay of implanted ^{74}Cu ions were detected in SuN in coincidence with the β -decay electron in the DSSD within a 1-s window. The much longer half-life of the daughter, ^{74}Zn (95.6 s), compared to the parent, ^{74}Cu (1.63 s), allowed for the ^{74}Zn decay to be excluded

from the analysis. The half-life of ^{74}Cu was confirmed by fitting the time between the arrival of the ion at the end station and the detection of the β -decay electron, which resulted in a half-life of 1.62(5) s that agrees well with the accepted value [25,26]. The randomly correlated background was obtained by performing the correlation between the ion and β -decay electron backwards in time [27].

The NLD and γ SF for ^{74}Zn were extracted from the experimental data using the β -Oslo method, which combines the traditional Oslo analysis [28,29] with β decay and total absorption spectroscopy. This allows the method to be applied further from stability and at lower beam rates than reaction-based methods and has been successfully used to constrain the neutron-capture rates of a number of neutron-rich nuclei in the $A \approx 80$ region [14,15,23]. The β -Oslo method uses the β decay to populate highly excited states in the daughter nucleus, which then de-excites through the emission of γ rays. The application of the β -Oslo technique requires information on both the excitation energy of the nucleus populated in β decay (E_x) and the individual γ -ray energies emitted in the de-excitation to the ground state (E_γ). The excitation energy is obtained from the total energy detected in SuN, while the individual γ -ray energies are obtained from the energy detected in each of the single segments of SuN. There are four main steps to obtain the experimental NLD and γ SF used to infer the neutron-capture cross section starting from a raw E_x vs. E_γ matrix: (1) unfolding of the raw γ -ray spectrum for each excitation energy [30], (2) isolation of the primary γ rays [28], (3) extraction of the functional forms of the NLD and γ SF [29], and (4) normalization of the NLD and γ SF [30,31].

III. RESULTS AND DISCUSSION

A. β -Oslo analysis

The raw, unfolded, and primary E_x vs. E_γ matrices following the β decay of ^{74}Cu are shown in Fig. 1. The response of SuN was modeled in GEANT4 [32], validated against experimental data, and used to unfold the raw matrix. An iterative subtraction method was used to isolate the primary γ -ray matrix, which contains only the distribution of the first γ rays to leave each excitation energy [28]. This distribution can be used to describe the probability of emitting a γ ray of a given energy as a function of excitation energy using the following proportionality:

$$P(E_x, E_\gamma) \propto \rho(E_x - E_\gamma) \times \mathcal{T}(E_\gamma), \quad (1)$$

where $\rho(E_x - E_\gamma)$ is the NLD at the excitation energy of the nucleus after emission of the γ ray and $\mathcal{T}(E_\gamma)$ is the transmission coefficient of the γ ray. The transmission coefficient can be transformed into the γ SF, assuming dipole transitions, using the simple relationship

$$f(E_\gamma) = \frac{\mathcal{T}(E_\gamma)}{2\pi E_\gamma^3}. \quad (2)$$

The NLD and $\mathcal{T}(E_\gamma)$ functions were extracted simultaneously from the primary matrix in the range $E_x \in [4.0, 8.0]$ MeV and $E_{\gamma, \text{min}} = 1.4$ MeV [29]. By an iterative χ^2 minimization procedure, a unique solution of the functional forms

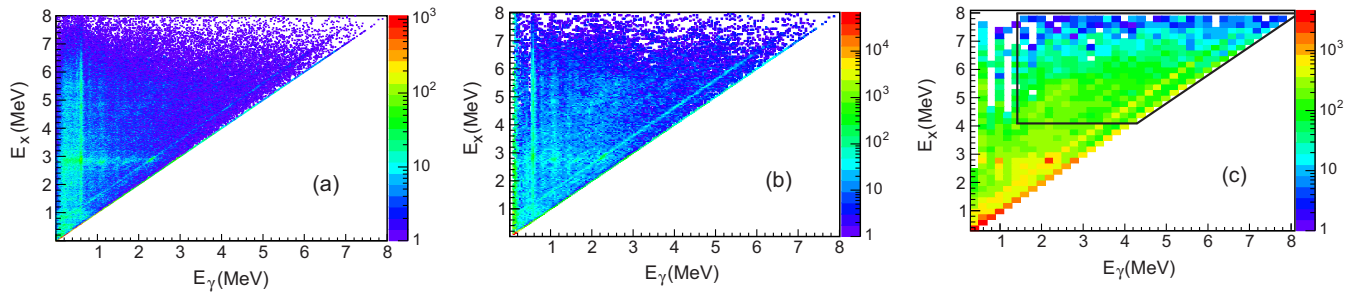


FIG. 1. (a) Raw E_x vs. E_γ matrix from the β decay of ^{74}Cu , with 20 keV/channel binning. (b) Unfolded matrix with 40 keV/channel binning. (c) Primary matrix with 200 keV/channel binning. The black box outlines the E_x, E_γ ranges used in the NLD and γSF extraction.

of the NLD and $\mathcal{T}(E_\gamma)$ were obtained. Two pieces of information are needed to normalize the NLD: the low-energy level density and the level density at the neutron separation energy [$\rho(S_n)$], which is 8.235 MeV for ^{74}Zn . The low-energy level density was determined using the known levels in ENSDF for ^{74}Zn and was assumed to be complete up to 3 MeV. There is no experimental data for $\rho(S_n)$, so a tabulated NLD [33] was used and shifted in energy to match the low-energy levels. The energy shift had a value of 0.4 ± 0.2 MeV, resulting in a $\rho(S_n)$ of 5200 MeV^{-1} , with upper and lower values of 6360 and 4230 MeV^{-1} , respectively. Another tabulated level density [34] did not differ significantly from the one used, and the generalized super fluid model (GSM) [35], which has been investigated for other nuclei, does not offer parameters for ^{74}Zn .

β decay populates a narrow spin range in the daughter isotope, which must be taken into account in the normalization. The ground state of ^{74}Cu is 2^- [36] which leads to the range of spins 0–4, of both parities, being populated in the daughter nucleus (^{74}Zn) following an allowed β decay and one dipole photon transition. The spin distribution around $\rho(S_n)$ from the tabulated NLD in Ref. [33] is shown in Fig. 2, with the spins populated following β decay and one dipole photon transition

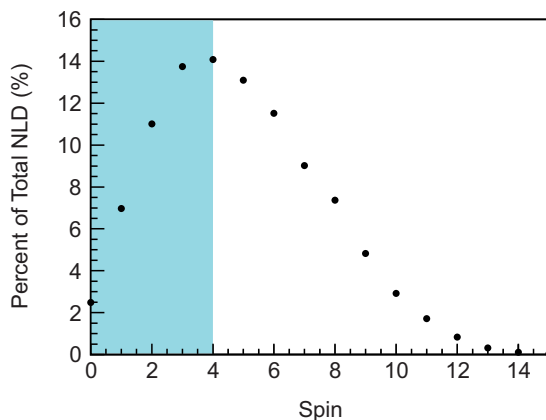


FIG. 2. Distribution of spins for the levels in ^{74}Zn around the neutron separation energy based on tabulated spin-dependent level densities from Ref. [33]. Spins highlighted in blue are populated following the β decay of ^{74}Cu and one dipole photon transition. The ground state of ^{74}Cu is 2^- [36].

highlighted in blue. This spin range corresponds to 48% of the total level density at the neutron separation energy, leading to reduced $\rho(S_n)$ upper, middle, and lower values of 3070, 2510, and 2040 MeV^{-1} , respectively.

The γSF was normalized to photoabsorption cross-section data from the nearby stable nuclei ^{70}Zn and $^{74,76}\text{Ge}$ [37]. Each data set was fit with a generalized Lorentzian (GLO) function [38] and extrapolated down in energy to 4 MeV. The giant dipole resonance (GDR) parameters obtained from the GLO fits to each nucleus are shown in Table I. The experimental γSF was scaled to obtain a χ^2 minimum with the fit of the extrapolated GLO function. The normalized NLD and γSF are shown in Fig. 3.

B. Cross section and reaction rate determination

The normalized NLD and γSF were used as inputs in TALYS to calculate the neutron-capture cross section and reaction rate. The normalized γSF was fit with a GLO function using the GDR parameters from the GLO fits to the photoabsorption data (see Table I) and an exponential function to account for the increase in the γSF at low γ -ray energies [39], with a constant value of $1.02_{-1.02}^{+1.24} \times 10^{-7} \text{ MeV}^{-3}$ and a slope of $1.6(7) \text{ MeV}^{-1}$.

The neutron-capture cross section and reaction rate are shown in Fig. 4. The lighter, larger bands show the range for both the cross section and reaction rate when using all combinations of NLD and γSF available in TALYS, excluding the temperature-dependent Hartree-Fock-Bogoliubov (HFB) level density [40] and the Brink-Axel single Lorentzian formula for the γSF [41,42]. Odd-even effects on neutron-capture rates away from stability were enhanced when using the temperature-dependent HFB level density [14] and have

TABLE I. GDR parameters from GLO fits to experimental data from Ref. [37]. E_{E1} is the energy of the giant resonance, Γ_{E1} is the width, and σ_{E1} is the strength. A value of 0.7 for T_f in the GLO function was adopted for all three data sets.

Nucleus	E_{E1} (MeV)	σ_{E1} (mb)	Γ_{E1} (MeV)
^{70}Zn	17.64(6)	97(1)	9.9(2)
^{74}Ge	17.86(10)	95(1)	12.4(4)
^{76}Ge	17.64(9)	101(1)	11.2(4)

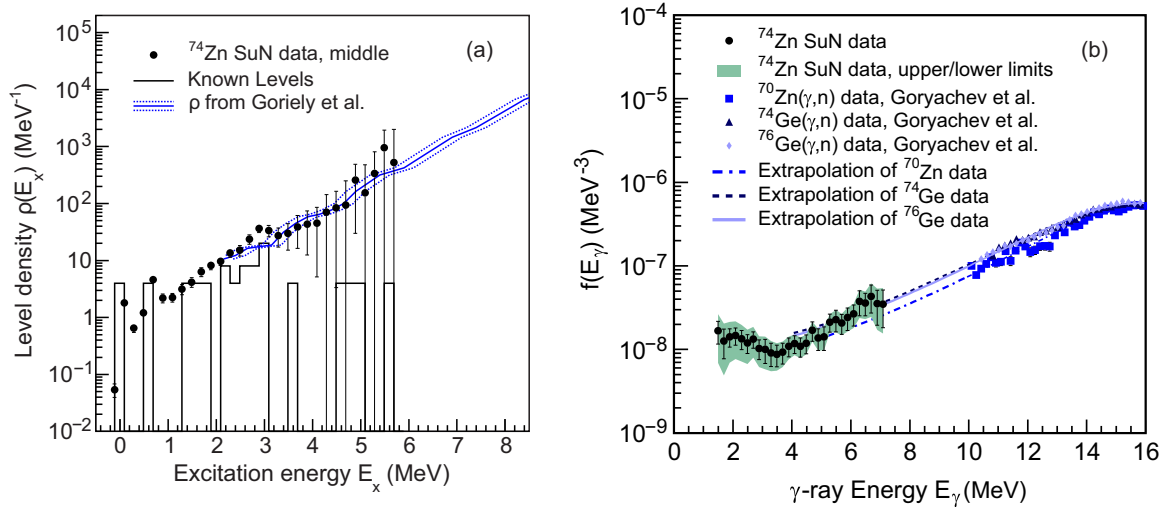


FIG. 3. (a) Nuclear level density for ^{74}Zn showing the experimental data (black circles), known levels from NNDC (solid black line), and level density calculated in Ref. [33] using the Hartree-Fock-Bogoliubov plus combinatorial method (solid blue line, see text for details). Dashed blue lines indicate uncertainties on the shift of the calculated level density. (b) Gamma strength function for ^{74}Zn showing the experimental data (black circles), experimental data for ^{70}Zn and $^{74,76}\text{Ge}$ from Ref. [37] (blue squares, triangles, and diamonds), and the GLO fit to that data and extrapolation to lower energies (blue solid, dashed, and dot-dashed lines). The last 15 points of the experimental γ SF were used to minimize the distance between the experimental γ SF and the extrapolations of the (γ, n) data sets. The green band indicates the combined statistical and systematic uncertainty.

been shown to differ from the almost exponential behavior seen in level-density experiments [40,43,44]. Additionally, the Brink-Axel single Lorentzian γ SF formula overestimates experimental neutron-capture cross sections of stable nuclei (for example, Refs. [38,45]). For all cases the default OMP, from Koning and Delaroche, was used [46]. The Jeukenne-Lejeune-Mahaux (JLM) semimicroscopic OMP [47] was also investigated, and the results were within 5% of the Koning and Delaroche OMP. A reduction of approximately 40% in the uncertainty can be achieved by only using NLD models that fall within the $\rho(S_n)$ normalization point and renormalizing the γ SF models using the same procedure as described for the experimental data. A further approximate 30% reduction

is obtained in the $^{73}\text{Zn}(n, \gamma)^{74}\text{Zn}$ cross-section uncertainty using the experimental data, resulting in an uncertainty of under a factor of 2, as shown with the darker bands.

The uncertainty presented here is specific to a cross section and reaction rate obtained from TALYS using experimental data. However, TALYS is not the only Hauser-Feshbach statistical model code available to determine neutron-capture cross sections. It is not feasible to compare neutron-capture cross sections obtained from different codes for every nucleus where an experimental NLD and γ SF has been extracted, so it is important to understand there is a broader uncertainty to these calculations that is extremely difficult to quantify.

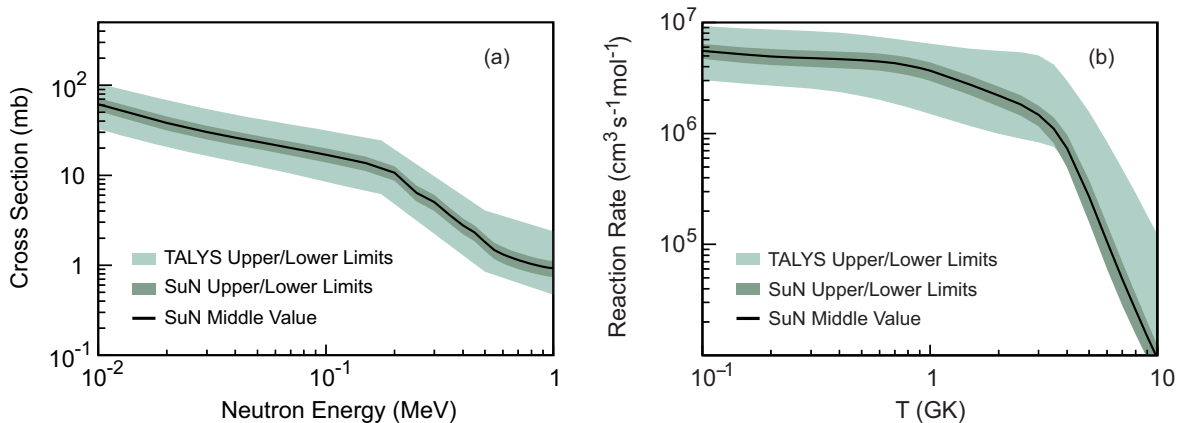


FIG. 4. (a) Cross section for the $^{73}\text{Zn}(n, \gamma)^{74}\text{Zn}$ reaction calculated in TALYS. The lighter band shows the variation in the cross section resulting from combinations of the available NLD and γ SF options in TALYS. The darker band shows the uncertainty in the cross section when using the experimental NLD and γ SF. (b) Astrophysical reaction rate calculated by TALYS. The lighter and darker bands are the same as for the cross-section calculation.

For the purpose of comparison, the systematic uncertainty inherent to the choice of Hauser-Feshbach code does not have an impact. Using the β -Oslo method and TALYS to infer neutron-capture cross sections for many nuclei in the $A \approx 80$ region will allow for comparisons across neutron and proton numbers of NLDs, γ SFs, and cross sections. Having a deeper understanding of the systematic changes to the NLD and γ SF, especially, will make predicting neutron-capture cross sections very far from stability more robust.

IV. CONCLUSIONS

The cross section and reaction rate for $^{73}\text{Zn}(n, \gamma)^{74}\text{Zn}$ have been experimentally constrained using the β -Oslo method. The NLD and γ SF of ^{74}Zn were extracted from the β decay of ^{74}Cu and provide the first experimental measurements of these properties. A reduction in the uncertainty of both the neutron-capture cross section and reaction rate to under a

factor of 2 in TALYS was obtained, which will add to nuclei in the $A \approx 80$ region that are used in astrophysical models with small uncertainties.

ACKNOWLEDGMENTS

This work was supported by the National Science Foundation under Grants No. PHY 1350234 (CAREER), No. PHY 1102511 (NSCL), No. PHY 1404442, and No. PHY 0822648 (Joint Institute for Nuclear Astrophysics). We also acknowledge the support of the Department of Energy National Nuclear Security Administration (NNSA) under Grants No. DE-NA0003221 and No. DE-NA0002132, and the Nuclear Science and Security Consortium under Awards No. DE-NA0000979 and No. DE-NA0003180. A.C. acknowledges support under DOE Contract No. DE-AC52-06NA25396. A.C.L. gratefully acknowledges funding through ERC-STG-2014, Grant No. 637686.

-
- [1] E. M. Burbidge, G. R. Burbidge, W. A. Fowler, and F. Hoyle, *Rev. Mod. Phys.* **29**, 547 (1957).
- [2] A. G. W. Cameron, *Publ. Astron. Soc. Pac.* **69**, 201 (1957).
- [3] D. Kasen, B. Metzger, J. Barnes, E. Quataert, and E. Ramirez-Ruiz, *Nature* **551**, 80 (2017).
- [4] M. R. Drout, A. L. Piro, B. J. Shappee, C. D. Kilpatrick, J. D. Simon, C. Contreras, D. A. Coulter, R. J. Foley, M. R. Siebert, N. Morrell, K. Boutsia, F. Di Mille, T. W. Holoién, D. Kasen, J. A. Kollmeier, B. F. Madore, A. J. Monson, A. Murguía-Berthier, Y. C. Pan, J. X. Prochaska, E. Ramirez-Ruiz, A. Rest, C. Adams, K. Alatalo, E. Bañados, J. Baughman, T. C. Beers, R. A. Bernstein, T. Bitsakis, A. Campillay, T. T. Hansen, C. R. Higgs, A. P. Ji, G. Maravelias, J. L. Marshall, C. Moni Bidin, J. L. Prieto, K. C. Rasmussen, C. Rojas-Bravo, A. L. Strom, N. Ulloa, J. Vargas-González, Z. Wan, and D. D. Whitten, *Science* **358**, 1570 (2017).
- [5] S. Wanajo, H. T. Janka, and B. Müller, *Astrophys. J. Lett.* **726**, L15 (2011).
- [6] R. Surman, M. Mumpower, R. Sinclair, K. L. Jones, W. R. Hix, and G. C. McLaughlin, *AIP Adv.* **4**, 041008 (2014).
- [7] J. Cowan and W. Rose, *Astrophys. J.* **212**, 149 (1977).
- [8] C. Sneden, J. J. Cowan, and R. Gallino, *Ann. Rev. Astron. Astrophys.* **46**, 241 (2008).
- [9] M. R. Mumpower, R. Surman, G. C. McLaughlin, and A. Aprahamian, *Prog. Part. Nucl. Phys.* **86**, 86 (2016).
- [10] M. Arnould, S. Goriely, and K. Takahashi, *Phys. Rep.* **450**, 97 (2007).
- [11] W. Hauser and H. Feshbach, *Phys. Rev.* **87**, 366 (1952).
- [12] S. I. Al-Quraishi, S. M. Grimes, T. N. Massey, and D. A. Resler, *Phys. Rev. C* **63**, 065803 (2001).
- [13] D. Savran, T. Aumann, and A. Zilges, *Prog. Part. Nucl. Phys.* **70**, 210 (2013).
- [14] S. N. Liddick, A. Spyrou, B. P. Crider, F. Naqvi, A. C. Larsen, M. Guttormsen, M. Mumpower, R. Surman, G. Perdikakis, D. L. Bleuel, A. Couture, L. Crespo Campo, A. C. Dombos, R. Lewis, S. Mosby, S. Nikas, C. J. Prokop, T. Renstrom, B. Rubio, S. Siem, and S. J. Quinn, *Phys. Rev. Lett.* **116**, 242502 (2016).
- [15] A. Spyrou, S. N. Liddick, A. C. Larsen, M. Guttormsen, K. Cooper, A. C. Dombos, D. J. Morrissey, F. Naqvi, G. Perdikakis, S. J. Quinn, T. Renstrøm, J. A. Rodriguez, A. Simon, C. S. Sumithrarachchi, and R. G. T. Zegers, *Phys. Rev. Lett.* **113**, 232502 (2014).
- [16] J. E. Escher, J. T. Burke, F. S. Dietrich, N. D. Scielzo, I. J. Thompson, and W. Younes, *Rev. Mod. Phys.* **84**, 353 (2012).
- [17] J. Cizewski, R. Hatarik, K. Jones, S. Pain, J. Thomas, M. Johnson, D. Bardayan, J. Blackmon, M. Smith, and R. Kozub, *Nucl. Instrum. Methods A* **261**, 938 (2007).
- [18] H. Utsunomiya, S. Goriely, H. Akimune, H. Harada, F. Kitatani, S. Goko, H. Toyokawa, K. Yamada, T. Kondo, O. Itoh, M. Kamata, T. Yamagata, Y.-W. Lui, I. Daoutidis, D. P. Arteaga, S. Hilaire, and A. J. Koning, *Phys. Rev. C* **82**, 064610 (2010).
- [19] A. Koning, S. Hilaire, and M. Duijvestijn, in *TALYS-1.6: Proceedings of the International Conference on Nuclear Data for Science and Technology 2007* (EDP Sciences, Nice, France, 2007).
- [20] A. J. Koning and D. Rochman, *Nucl. Data Sheets* **113**, 2841 (2012).
- [21] D. J. Morrissey, B. M. Sherrill, M. Steiner, A. Stolz, and I. Wiedenhoever, *Nucl. Instrum. Methods B* **204**, 90 (2003).
- [22] A. Spyrou, S. N. Liddick, F. Naqvi, B. P. Crider, A. C. Dombos, D. L. Bleuel, B. A. Brown, A. Couture, L. Crespo Campo, M. Guttormsen, A. C. Larsen, R. Lewis, P. Möller, S. Mosby, M. R. Mumpower, G. Perdikakis, C. J. Prokop, T. Renstrøm, S. Siem, S. J. Quinn, and S. Valenta, *Phys. Rev. Lett.* **117**, 142701 (2016).
- [23] A. Spyrou, A. C. Larsen, S. N. Liddick, F. Naqvi, B. P. Crider, A. C. Dombos, M. Guttormsen, D. L. Bleuel, A. Couture, L. Crespo Campo, R. Lewis, S. Mosby, M. R. Mumpower, G. Perdikakis, C. J. Prokop, S. J. Quinn, T. Renstrøm, S. Siem, and R. Surman, *J. Phys. G* **44**, 044002 (2017).
- [24] A. Simon, S. J. Quinn, A. Spyrou, A. Battaglia, I. Beskin, A. Best, B. Bucher, M. Couder, P. A. Deyoung, X. Fang, J. Görres, A. Kontos, Q. Li, S. N. Liddick, A. Long, S. Lyons, K. Padmanabhan, J. Peace, A. Roberts, D. Robertson, K. Smith, M. K. Smith, E. Stech, B. Stefanek, W. P. Tan, X. D. Tang, and M. Wiescher, *Nucl. Instrum. Methods A* **703**, 16 (2013).
- [25] J. A. Winger, J. C. Hill, F. K. Wohn, E. K. Warburton, R. L. Gill, A. Piotrowski, and D. S. Brenner, *Phys. Rev. C* **39**, 1976 (1989).

- [26] J. Van Roosbroeck, H. De Witte, M. Gorska, M. Huyse, K. Kruglov, D. Pauwels, J. C. Thomas, K. Van De Vel, P. Van Duppen, S. Franchoo, J. Cederkall, V. N. Fedoseyev, H. Fynbo, U. Georg, O. Jonsson, U. Köster, L. Weissman, W. F. Mueller, V. I. Mishin, D. Fedorov, A. De Maesschalck, N. A. Smirnova, and K. Heyde, *Phys. Rev. C* **71**, 054307 (2005).
- [27] T. Kurtukian-Nieto, J. Benlliure, and K. H. Schmidt, *Nucl. Instrum. Methods A* **589**, 472 (2008).
- [28] M. Guttormsen, T. Ramsøy, and J. Rekstad, *Nucl. Instrum. Methods A* **255**, 518 (1987).
- [29] A. Schiller, L. Bergholt, M. Guttormsen, E. Melby, J. Rekstad, and S. Siem, *Nucl. Instrum. Methods A* **447**, 498 (2000).
- [30] M. Guttormsen, T. S. Tveter, L. Bergholt, F. Ingebretsen, and J. Rekstad, *Nucl. Instrum. Methods A* **374**, 371 (1996).
- [31] A. C. Larsen, M. Guttormsen, M. Krτίčka, E. Běťák, A. Bürger, A. Görge, H. T. Nyhus, J. Rekstad, A. Schiller, S. Siem, H. K. Toft, G. M. Tveten, A. V. Voinov, and K. Wikan, *Phys. Rev. C* **83**, 034315 (2011).
- [32] J. Allison, K. Amako, J. Apostolakis, P. Arce, M. Asai, T. Aso, E. Bagli, A. Bagulya, S. Banerjee, G. Barrand, B. R. Beck, A. G. Bogdanov, D. Brandt, J. M. Brown, H. Burkhardt, P. Canal, D. Cano-Ott, S. Chauvie, K. Cho, G. A. Cirrone, G. Cooperman, M. A. Cortés-Giraldo, G. Cosmo, G. Cuttone, G. Depaola, L. Desorgher, X. Dong, A. Dotti, V. D. Elvira, G. Folger, Z. Francis, A. Galoyan, L. Garnier, M. Gayer, K. L. Genser, V. M. Grichine, S. Guatelli, P. Guèye, P. Gumplinger, A. S. Howard, I. Hřivnáčová, S. Hwang, S. Incerti, A. Ivanchenko, V. N. Ivanchenko, F. W. Jones, S. Y. Jun, P. Kaitaniemi, N. Karakatsanis, M. Karamitrosi, M. Kelsey, A. Kimura, T. Koi, H. Kurashige, A. Lechner, S. B. Lee, F. Longo, M. Maire, D. Mancusi, A. Mantero, E. Mendoza, B. Morgan, K. Murakami, T. Nikitina, L. Pandola, P. Paprocki, J. Perl, I. Petrović, M. G. Pia, W. Pokorski, J. M. Quesada, M. Raine, M. A. Reis, A. Ribon, A. Ristić Fira, F. Romano, G. Russo, G. Santin, T. Sasaki, D. Sawkey, J. I. Shin, I. I. Strakovsky, A. Taborda, S. Tanaka, B. Tomé, T. Toshito, H. N. Tran, P. R. Truscott, L. Urban, V. Uzhinsky, J. M. Verbeke, M. Verderi, B. L. Wendt, H. Wenzel, D. H. Wright, D. M. Wright, T. Yamashita, J. Yarba, and H. Yoshida, *Nucl. Instrum. Methods A* **835**, 186 (2016).
- [33] S. Goriely, S. Hilaire, and A. J. Koning, *Phys. Rev. C* **78**, 064307 (2008).
- [34] S. Goriely, F. Tondeur, and J. Pearson, *At. Data Nucl. Data Tables* **77**, 311 (2001).
- [35] A. V. Ignatyuk, J. L. Weil, S. Raman, and S. Kahane, *Phys. Rev. C* **47**, 1504 (1993).
- [36] K. T. Flanagan, P. Vingerhoets, M. L. Bissell, K. Blaum, B. A. Brown, B. Cheal, M. De Rydt, D. H. Forest, C. Geppert, M. Honma, M. Kowalska, J. Krämer, A. Krieger, E. Mané, R. Neugart, G. Neyens, W. Nörtershäuser, M. Schug, H. H. Stroke, and D. T. Yordanov, *Phys. Rev. C* **82**, 041302(R) (2010).
- [37] A. Goryachev and G. Zalesnyy, *Vopr. Teor. Yad. Fiz.* **8**, 121 (1982).
- [38] J. Kopecky and M. Uhl, *Phys. Rev. C* **41**, 1941 (1990).
- [39] R. Schwengner, S. Frauendorf, and A. C. Larsen, *Phys. Rev. Lett.* **111**, 232504 (2013).
- [40] S. Hilaire, M. Girod, S. Goriely, and A. J. Koning, *Phys. Rev. C* **86**, 064317 (2012).
- [41] D. Brink, *Nucl. Phys.* **4**, 215 (1957).
- [42] P. Axel, *Phys. Rev.* **126**, 671 (1962).
- [43] A. V. Voinov, B. M. Oginni, S. M. Grimes, C. R. Brune, M. Guttormsen, A. C. Larsen, T. N. Massey, A. Schiller, and S. Siem, *Phys. Rev. C* **79**, 031301 (2009).
- [44] M. Guttormsen, B. Jurado, J. N. Wilson, M. Aiche, L. A. Bernstein, Q. Ducasse, F. Giacoppo, A. Görge, F. Gunsing, T. W. Hagen, A. C. Larsen, M. Lebois, B. Leniau, T. Renstrøm, S. J. Rose, S. Siem, T. Tornyi, G. M. Tveten, and M. Wiedeking, *Phys. Rev. C* **88**, 024307 (2013).
- [45] R. Capote, M. Herman, P. Obložinský, P. G. Young, S. Goriely, T. Belgya, A. V. Ignatyuk, A. J. Koning, S. Hilaire, V. A. Plujko, M. Avrigeanu, O. Bersillon, M. B. Chadwick, T. Fukahori, Z. Ge, Y. Han, S. Kailas, J. Kopecky, V. M. Maslov, G. Reffo, M. Sin, E. S. Soukhovitskii, and P. Talou, *Nucl. Data Sheets* **110**, 3107 (2009).
- [46] A. J. Koning and J. P. Delaroche, *Nucl. Phys. A* **713**, 231 (2003).
- [47] J.-P. Jeukenne, A. Lejeune, and C. Mahaux, *Phys. Rev.* **15**, 10 (1977).